A new concept of hybrid solar collectors: Polymeric heat exchanger for photovoltaic panels

Victor C. Pigozzo Filho[1,2], Bruna de O. Busson[1,2], Alexander Leyton M.[1,2], Alex C. Santos[2], Daniel S. Gomide[2], Loic Tachon[3], Felipe C. de Araújo[1], Henrique Hipólito[3], Júlio C. Passos[2] and Mateus A. Gabiatti[4]

[1] Advanced Institute of Technology and Innovation (IATI), Recife (Brazil)

[2] Federal University of Santa Catarina, Florianópolis (Brazil)

[3] Soluz Energia, Florianópolis (Brazil)

[4] Engie Brasil Energia, Florianópolis (Brazil)

Abstract

Hybrid solar collectors generate electricity and heat at the same device. The present paper proposes a new concept of heat exchanger to be used in conventional photovoltaic (PV) modules, converting them into hybrid collectors. The proposed heat exchanger is made of corrugated polypropylene sheets, with multiple channels that occupies the full width of the PV module bottom surface. To characterize it, an experimental test bench was developed and numerical simulations using EES software were performed. The objective is to assess the heat exchanger performance and to attest that the energy balance modeling is suitable to predict the amount of heat flux absorbed by water. After carrying out experimental test configurations, the thermal contact resistance between the heat exchanger and the PV surface of 0.008 m^2 K W^{-1}. The deviation between measured and calculated heat fluxes are about 12% and 8% for configurations without and with bottom thermal insulation, respectively.

Keywords: Hybrid solar collector, PVT modules, Polymeric heat exchanger, Heat transfer analysis

1. Introduction

Photovoltaic (PV) solar energy is obtained by the transformation of solar radiation into electrical energy using solar cells constructed with semiconductor materials, reaching efficiencies between 14% and 22% in commercially available panels (Blakesley et al., 2020). PV efficiency is defined by how effective the solar conversion process in electrical energy is (Pinho and Galdino, 2014). Nonetheless, there is a negative linear dependence on the efficiency of the PV panel with the increase of the operating temperature (Dubey et al., 2013). A cooling system can be adopted for the PV panels to counteract the loss of efficiency due to the temperature increase, and even, at the same time can harvest the rejected heat (Zarrella et al., 2019).

Different approaches exist for PV cooling, in active and passive ways, in the pursuit of reducing PV operating temperature and consequently increasing the PV conversion efficiency (Busson et al., 2021). The hybrid, or photovoltaic thermal (PVT), system generates electricity and supplies buildings with thermal energy while removing heat from the PV panel (Huide et al., 2017; Sultan and Efzan, 2018). The PVT modules may be cooled by water spray jets (Da Rocha et al., 2019) or by a heat exchanger, where a heat transfer fluid circulates, in contact with the rear face of solar cells (Preet, 2018). There are still options to remove heat from the PV module such as to submerge PV modules in water reservoirs, lakes, or rivers (Enaganti et al., 2020) and to float PV modules over water tanks (Busson et al., 2021).

Unlike PV systems, which are intended to work at low temperatures to not compromise efficiency, in solar thermal systems the objective is to reach a high temperature, which varies according to the application (Suman et al., 2015). Therefore, the challenge involving PVT modules lies in the development of a thermally balanced hybrid system, optimizing electrical and thermal efficiencies (Shyam et al., 2015), and, thus, obtaining a global energy

doi:10.18086/swc.2021.22.07 Available at http://proceedings.ises.org

efficiency, thermal and electrical, higher than the two separate systems. Furthermore, the PVT efficiency depends on a combination of factors like working fluid, collector type, PV cells material, vitreous covering, flow configuration and heat exchanger type (Chow, 2010; Herrando et al., 2019).

Regarding working fluid, PVT can be cooled by air, water or other liquid. Despite the natural air circulation making the system cooling cheaper and simpler, it is less efficient in regions where the ambient temperature is typically higher than 20°C (Lamnatou and Chemisana, 2017), case of Brazil. In the case of PVs cooled by liquids circulating under their bottom surface, it is more common that water is used and flows through channels (Al-Waeli et al., 2019). Collectors cooled by water show better heat exchanger and lower PV operating temperature than collectors cooled by air (Moharram et al., 2013). However, a mixture with ethylene glycol is recommended in regions where temperatures below zero degrees are reached (Kazemian et al., 2018).

Concerning the heat exchangers used in hybrid collectors, two relevant parameters are the shape and amount of water flowing through channels. The absorber type can be sheet and tube, which is less costly, easier to manufacture, occupies less water capacity, or a thin channel below the full width of the PV rear surface, which enables a uniform temperature distribution, better heat transfer characteristics (Kumar et al., 2016). If multiple channels are chosen, then it may attain higher electrical and thermal efficiencies than sheet and tube configuration, however a good thermal contact between the absorber with multiple channels and PV bottom surface is harder to achieve (Kim and Kim, 2012a). Although, it has been determined that maximizing the transfer area is better than minimizing the contact resistance (Herrando et al., 2019). Each channel type can exhibit different shapes, like round, rectangular and others (Kim and Kim, 2012b; Kaewchoothong et al., 2021).

Most PVT manufacturers are European and produce uncovered water flat plate PVT collectors, the remaining is divided into 28% producing covered flat plate PVT collectors, 4% evacuated tube collector, 12% uncovered air flat plate collector and 8% concentrating PVT system (Ramschak, 2020).

The present paper introduces a new concept of a heat exchanger developed to be used in common PV panels, converting them into hybrid solar collectors. The proposed heat exchanger is made of corrugated polypropylene (PP) sheets and is installed at the rear face of the PV panel (Figure 1a). This heat exchanger is composed of 153 channels with a rectangular profile where water flows.

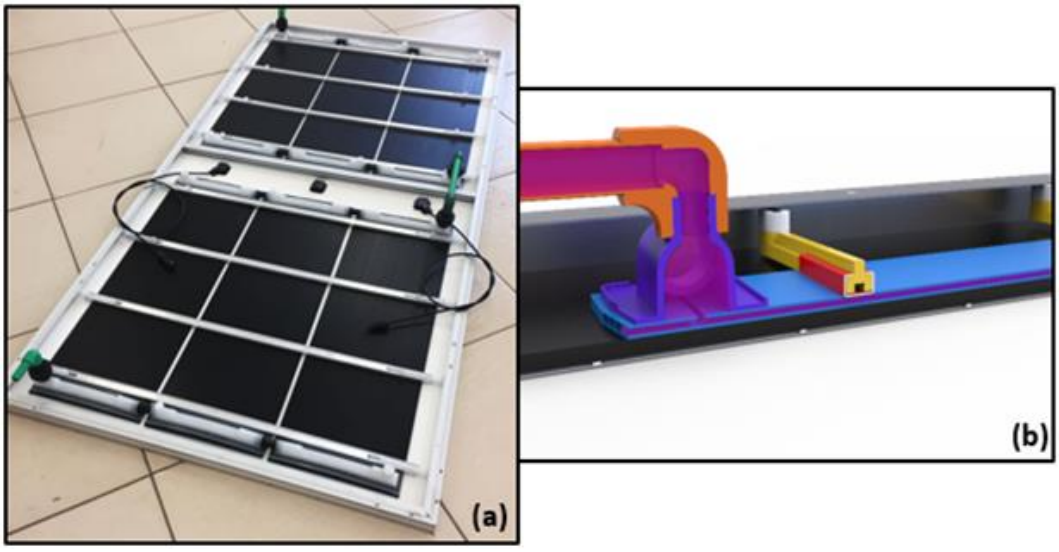

Fig. 1: New concept of heat exchanger installed on the PV module rear surface (a) and schematic representation of water circulation in the heat exchanger (b)

The main advantages of this system are the ability and the flexibility to convert any PV panel into a PVT panel and its low cost when compared to commercially available PVTs. The installation of the heat exchanger under the PV module rear surface is simple and fast, dismissing the use of extra tools where the PVT module will be located. Further the PP used to manufacture the heat exchanger is cheaper than other materials utilized commonly in PVTs and it is a suited material for long-term operation as solar collectors, like commercially available swimming pools

heating solar collectors.

Figure 1b shows the water, in purple, flowing through the components of the heat exchanger: inlet pipe, distribution manifold and the channels in the corrugated PP sheet. The heat exchanger is fastened by transversal cantilever springs. The cantilever springs fit under the aluminum frame of the PV module and mechanically fastens the heat exchanger without interfering with the PV module and can be easily installed or removed. In this way, no permanent modifications are made to the panel and therefore, terms of warranty can be maintained by manufacturers. This paper has the objective to assess, through experimental tests and simulations, the characteristics of the heat transfer in the proposed heat exchanger for PV modules.

2. Methodology

To characterize the corrugated PP sheet heat exchanger characteristics, an experimental test bench was developed and numerical simulations using Engineering Equation Solver (EES) software were performed. The experimental stage is an indoor test bench where the heat is supplied to the heat exchanger by means of electrical heaters located on the top of a thick aluminum plate. The aluminum plate has the function of uniformizing the heat flow that reaches the heat exchanger, approximating what occurs during the real conditions of PVT panels under solar radiation. Temperature and mass flow measurements were performed as well as the dissipated electrical power. The purpose of the experiments on this test bench is to identify the thermal losses in the novel heat exchanger under different heat fluxes and water inlet temperatures.

Figure 2 shows a schematic representation of the indoor experimental test bench installed at the LEPTEN laboratories at the Federal University of Santa Catarina (UFSC). The thermostatic water bath provides water at the desired test temperature. The pump and the valve are used to control the mass flow rate, which is measured by a Coriolis mass flow meter. Water enters the lowest level of the PVT heat exchanger and comes out at the highest level. The slope of PVT heat exchanger (ϕ angle in Figure 2) can be adjusted but in these tests was kept constant at 32°.

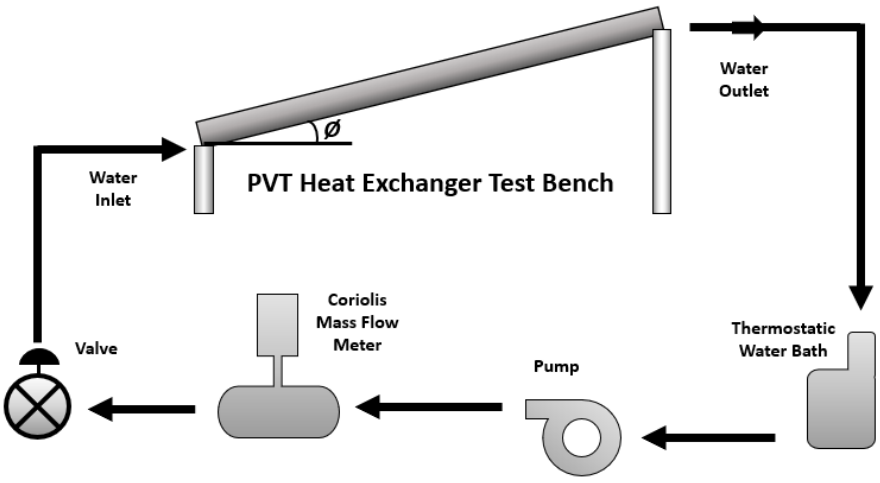

Fig. 2: Schematic illustration of the indoor test bench

Figure 3 presents a cross section of the PVT heat exchanger test bench. The electric heaters apply a heat flux over the aluminum plate, this flux is controlled by a DC power supply and is varied between 200 W m^{-2} and 800 W m^{-2}. The aluminum plate pretends to be the PV module and the heat exchanger under its surface fulfills the function of removing heat and delivers heat to water inside the corrugated PP sheet channels. To assess the heat exchanger effectiveness, not only the heat flux applied may be varied, but the water inlet temperature too. Three different water temperatures entering in heat exchanger channels were tested: 30 °C, 45 °C and 60 °C. Moreover, tests are carried out with and without the thermal insulation under the bottom heat exchanger surface.

Applications that demand water at temperatures higher than 40 °C, like domestic hot water heating, the bottom insulation must be used, although the PV module efficiency may be reduced. For applications that demand low

water temperatures, like pool heating, the bottom thermal insulation can be dismissed, and the PV module efficiency can be increased due to the cooling effect, depending on the water inlet temperature.

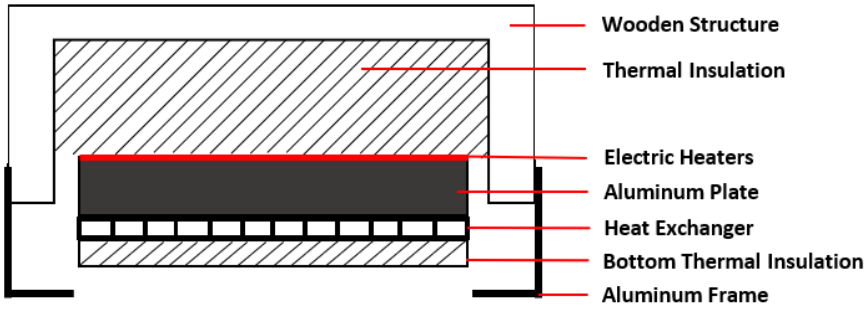

Fig. 3: PVT heat exchanger test bench cross section view

Figure 4 shows some details of the PVT test bench. Figure 4a shows the electric resistance installed on the top of the aluminum plate. Nickel chromium resistance strips were used with 22 mm between them, providing a uniform heat flux set at the bottom of the aluminum plate. Four aluminum plates of 300 mm wide and 450 mm long were used. All the nickel chromium strips are connected in series with a total electric resistance of 18 Ω. Figure 4b shows the aluminum plate bottom surface where the heat exchanger is installed. Figure 4c presents the test bench mounted with the heat exchanger installed.

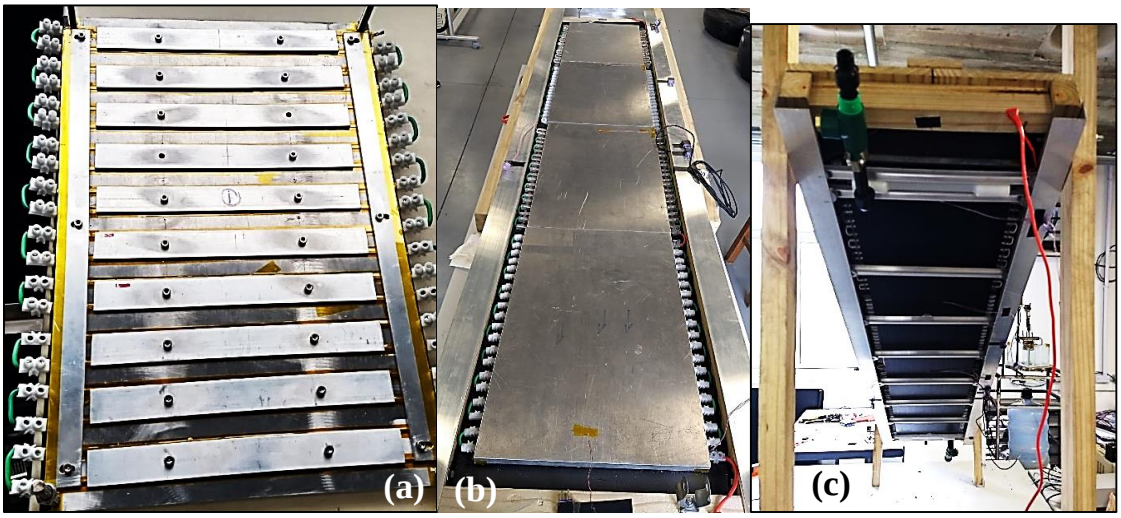

Fig. 4: PVT heat exchanger test bench aluminum plate with nickel chromium resistances (a), aluminum plate with uniform heat flux (b) and heat exchanger without bottom insulation (c)

The heat exchanger experimental results were used to validate a numerical model developed in the EES software. The EES algorithm is the one-dimensional heat exchanger energy balance discretization in steady state. The set of equations that compound the heat exchanger energy balance come from the energy balance between the nodes shown in Figure 5a. Figure 5b presents the correspondent thermal resistance circuit which connects the temperature nodes and energy fluxes.

The resistance between nodes 4 and 3 is the thermal contact resistance between the heat exchanger and the aluminum plate. This resistance indicates the quality of the heat exchanger fasten method and has a direct influence on the system performance. The vertical walls of the heat exchanger were considered adiabatic, once there are no temperature gradients in the horizontal direction. The heat flux from node 2 to 8 was considered by conduction through the PP vertical wall and by convection with the water (node 1). Radiation heat transfer occurs from surface 9 to the environment at ambient temperature. The radiation heat transfer was only considered for the

case of the system operating without bottom thermal insulation.

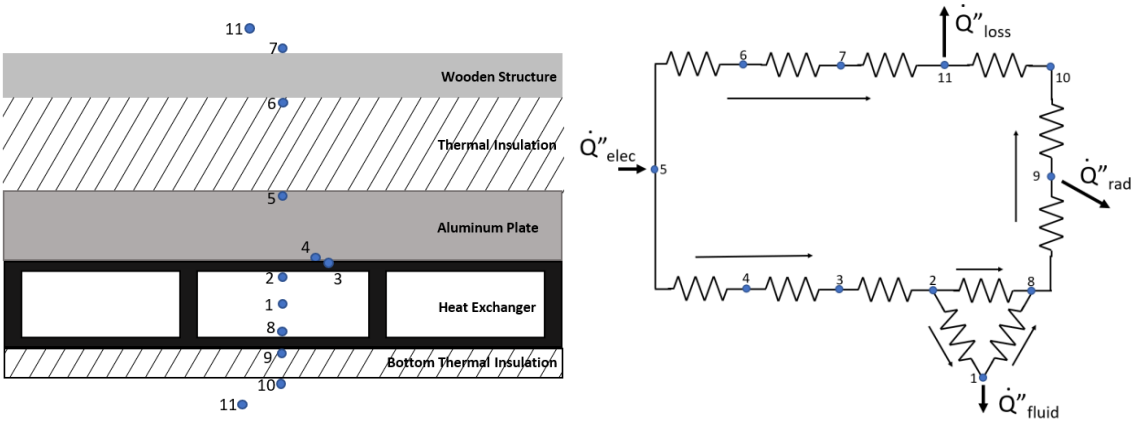

(a) **(b)**

Fig. 5: Node temperatures in the PVT heat exchanger test bench cross section view (a) and in thermal resistance circuit (b)

The heat exchanger width is 300 mm and the length is 1800 mm, with a total area of 0.54 m². The proposed heat exchanger used in the indoor test bench is composed of 44 rectangular channels with a hydraulic diameter equal to 4.24 mm. The mass flow rate was kept constant at 20 kg/h at every test and the ambient temperature near 20 °C. The input data for the model is the ambient temperature, water temperature and electric heat flux at node 5, as well as the components properties and dimensions, shown at Table 1.

Tab. 1: Properties and dimensions

Quantity	Value
Polypropylene thermal conductivity	0.21 W m^{-1} K^{-1}
Polypropylene emissivity	0.95
Insulation thermal conductivity	0.035 W m^{-1} K^{-1}
Aluminum thermal conductivity	240 W m^{-1} K^{-1}
Polypropylene thickness (nodes 3 to 4; 8 to 9)	0.8 mm
Insulation thickness	50 mm
Aluminum plate thickness	15.88 mm
Wood thickness	25 mm
Bottom insulation thickness	30 mm
Heat exchanger width	300 mm
Heat exchanger length	1800 mm
Number of channels	44

For determination of convection losses, it is important to define the convective heat transfer coefficient *h*. According to Duffie and Beckman (2006), the *h* acting on test bench upper and bottom surface (h_{1011}) is a combination of forced and natural convections:

$$h_{1011} = (h_{1011,nat}{}^{3} + h_{1011,forced}{}^{3})^{1/3} \quad \text{(eq. 1)}$$

$$h_{1011,nat} = 1.78\,(T_{10} - T_{11})^{1/3} \quad \text{(eq. 2)}$$

$$h_{1011,forced} = 2.8 + 3u_w \quad \text{(eq. 3)}$$

Where $h_{1011,nat}$ *is* the natural convection heat transfer coefficient, $h_{1011,forced}$ is the forced convection heat transfer coefficient, that is a linear function of the wind speed u_w, T_4 and T_{11} are the average surface and ambient temperatures, respectively. Besides, the inner channel convection coefficient (h_{28}) was calculated using a constant Nusselt number of 3.73, which is considered for rectangular tubes with laminar flow and nonuniform heat flux.

Figure 6a presents the PV module cross section with the heat exchanger installed and Figure 6b represents the heat transfer thermal circuit. This model considers that the solar radiation, *G*, reaches the surface 4 where PV cells are located, and it is converted into electrical and thermal energy. Surface 4 transfers the heat excess by radiation and conduction through the glass and the heat exchanger. The considered PV module on the simulations has a nominal PV efficiency (η_{0PV}) of 0.1811 and a power temperature coefficient of -0.37% K^{-1}. The electricity produced by the PV on the simulations depends on *G*, PV efficiency and T_4.

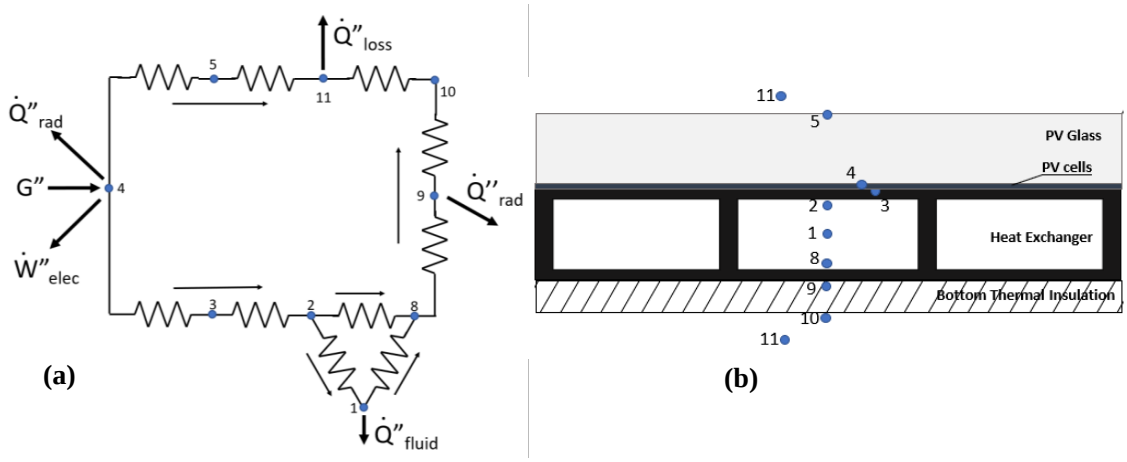

Fig. 6: Node temperatures in the PVT heat exchanger test bench cross section view (a) and in thermal resistance circuit (b)

The PV glass properties are transmittance-absorptance product, τα, of 0.90, thermal conductivity, k_{glass}, of 1.2 W m^{-1} K^{-1} and a thickness of 3.2 mm. The solar cells emissivity was considered 0.95. The radiation heat transfer from surface 4 was considered as exchanges with sky in an effective sky temperature 5 K less than the ambient temperature. The PV module without the heat exchanger installed on its rear surface was also simulated in the same way to obtain its electric power generation and operation temperatures to compare with the simulated PVT results.

3. Results

Figure 7 shows the comparison of the experimental and calculated results for the nodes temperatures 4, 5, 7 and 9, where thermocouples were installed. These node temperatures represent top and bottom aluminum plate surfaces and top and bottom surfaces that are exposed to forced convection induced by wind speed. When the node temperature values were plotted in Figure 7, it was possible to fit them and find out the thermal contact resistance that minimizes the experimental and calculated temperatures. The obtained value for the contact resistance was 0.008 m^2 K W^{-1}. This result will be employed in subsequent simulations in EES.

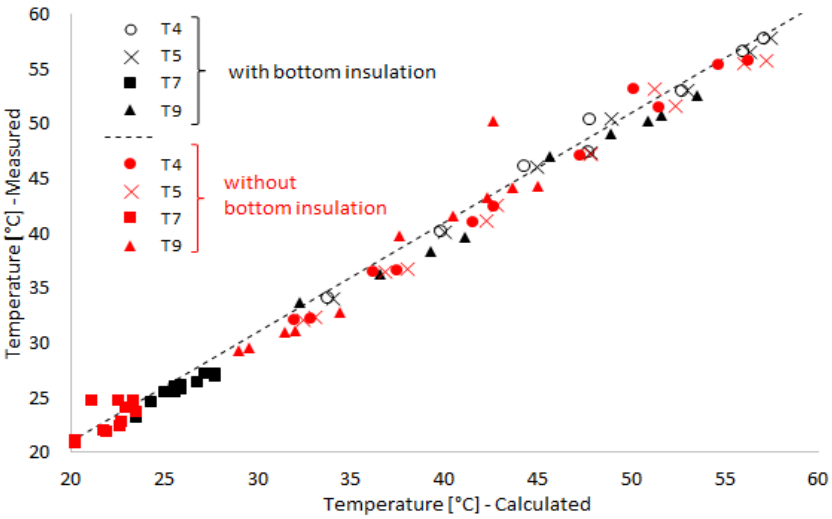

Fig. 7: Measured and calculated temperatures

Figure 8 presents a comparison between measured and calculated heat fluxes absorbed by the water. The error bars indicate the expanded uncertainty for the measured value, which is dependent on the temperature measurement uncertainty of 1% and the mass flow rate measurement uncertainty of 1%. It can be seen that almost all the experimental points in Figure 8 match the calculated ones considering its uncertainty interval. The negative values in Figure 8 represent the tests at high temperature in which the fluid loses more heat to the ambient than it gains from the electric resistance.

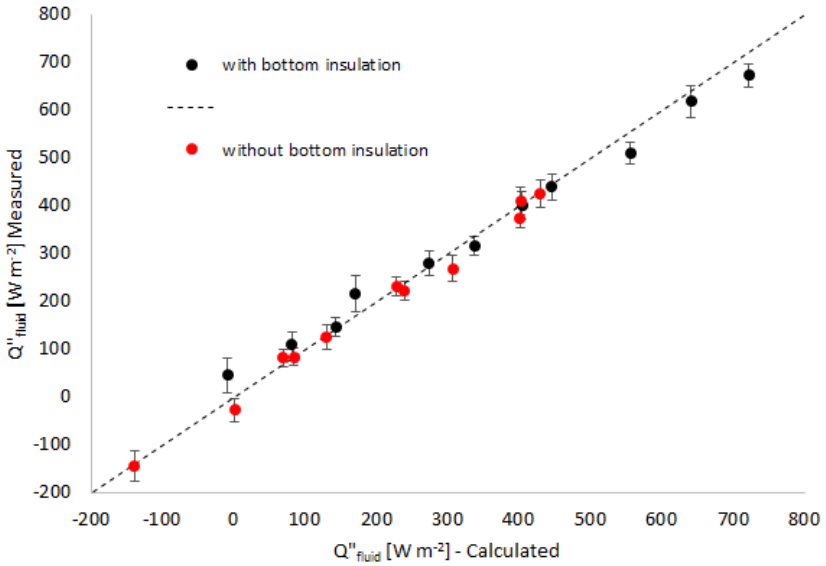

Fig. 8: Measured and calculated heat fluxes transferred to the water inside the heat exchanger

During experimental tests, the wind speed ranged from 0 m s^{-1} to 2 m s^{-1}, which applied in Equations 1 and 3 resulted in the values of the convection heat transfer coefficient from 3.71 W m^{-2} K^{-1} to 8.95 W m^{-2} K^{-1}.

Figure 9 shows the effect of thermal insulation on the amount of heat absorbed by water in presence of wind speed. Without bottom insulation, as wind speed increases more heat is lost by convection and less is collected by water, thus diminishing the heat exchanger performance. Nevertheless, when thermal insulation is installed in the heat exchanger rear surface the wind speed has a smaller influence on water heat absorption. Furthermore, as the

water inlet temperature increases the heat exchanger performance decreases due to a minor capacity of the fluid to absorb heat. The simulations presented in Figure 9 consider a heat flux at surface 4 of 400 W m^{-2}.

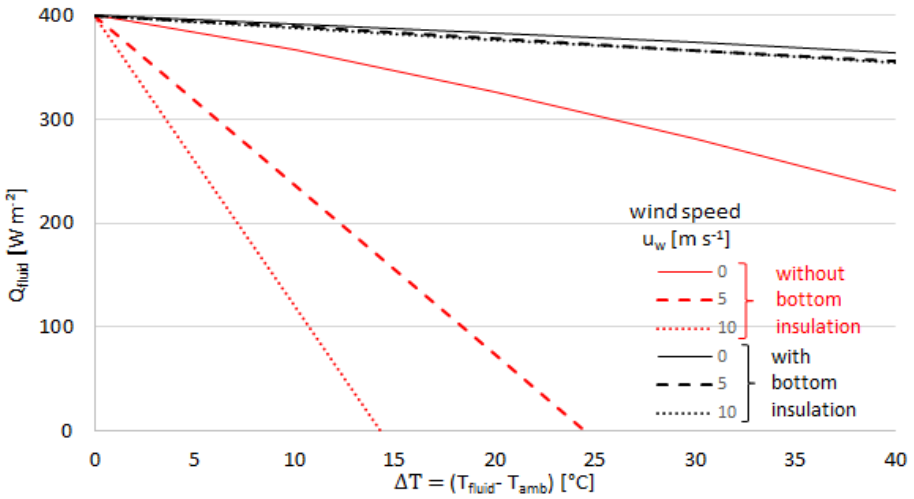

Fig. 9: Influence of wind speed on water heat absorption

The Reynolds number inside the PP channels ranged from 35 to 55 and h_{28} ranged from 530 to 555 W m^{-2} K^{-1}. The h_{28} was varied in simulations, but no significant influence on the results was observed.

With the thermal model validated by the test bench experimental results, the PVT model, presented in Figure 6, simulation results are now presented in some parametric analysis.

The electric power generation by the PV and PVT modules is presented in Figure 10. The PV generation is represented by the red curve. The PVT electric generation for three different fluid temperatures is represented by the black curves. The effect of PV efficiency improvement by using the heat exchanger is observed when water circulating inside the channels is at the lowest temperature considered, 25 ˚C, equal to the ambient temperature. On average, when water inlet temperature is equal to ambient temperature the PVT efficiency is 4% higher than PV efficiency achieving an efficiency improvement of 8% for maximum *G* level simulated. The wind speed in these simulations was maintained in 1 m s^{-1}. For PVT with water inlet temperature of 45 ˚C the efficiency is 1,5% lower than PV efficiency. When the water inlet temperature is 60 ˚C, PVT efficiency is 7% lower than the PV.

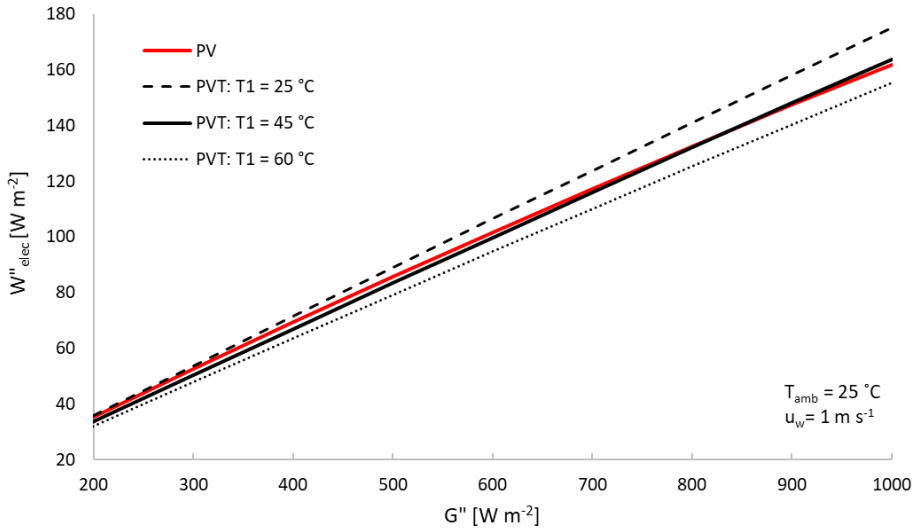

Fig. 10: Electric power generated for the PV only and PVTs with different water inlet temperatures

The solar cells temperatures (T_4) in the same cases of Figure 10 are represented in Figure 11. For water inlet temperatures of 45 °C and 60 °C, T_4 presents 51 °C and 63,5°C of maximum values, respectively. For water inlet temperature equal to 25 °C, T_4 is 29.4 °C reaching a maximum of 34,2 °C when G is 1000 W m^{-2}.

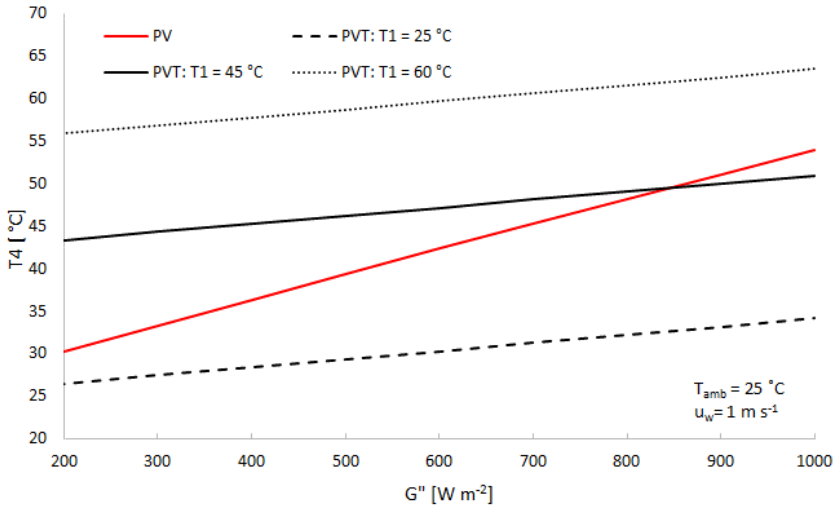

Fig. 11: Average cell temperature, T_4, of the PV and PVT with different water inlet temperatures

Figure 12 presents the thermal power generation of the PVT operating with different water inlet temperatures, without and with bottom thermal insulation. For the temperature of 25 ˚C, the PVT thermal generation in both cases are the same with a thermal efficiency in the range of 38% and 60% corresponding to a solar radiation of 100 W m^{-2} e 1000 W m^{-2}. As expected, the thermal generation decreases with the increase of the fluid temperature. For temperatures higher than 45 ˚C, when the PVT panel is operating under G levels of 700 W m^{-2} the heat losses are higher than the heat gained by water.

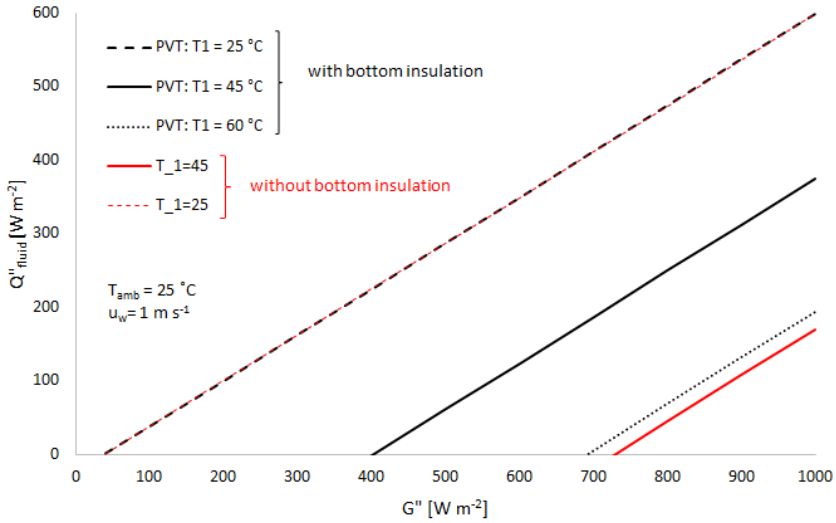

Fig. 12: PVT thermal energy generation when water inlet temperature and use of insulation change

Figure 13 presents the influence of thermal contact resistance on the PVT generation and on T_4. In this simulation, the solar irradiance was defined as 800 W m^{-2}, ambient temperature as 25 °C, wind speed as 1 m s^{-1} and water inlet temperature as 45 °C. Black curves depict PVT with bottom thermal insulation and red curves, PVT without thermal insulation. The blue line represents the value of 0.008 m^2 K W^{-1} for the thermal contact resistance obtained experimentally. The thermal and electrical energy generation deteriorates with the increase of the average solar

cell temperature. For contact resistances lower than 0.003 m^2 K W^{-1}, the PVT performance is almost constant. Above this value, the cell temperature starts to increase and it is most accentuated between 0.01 m^2 K W^{-1} and 0.1 m^2 K W^{-1}. The obtained value of 0.008 m^2 K W^{-1} can be considered at the limit of a region in which both drop in the solar cell temperatures and the thermal and electrical performances can be considered negligible, i.e., they are independent of the contact resistance.

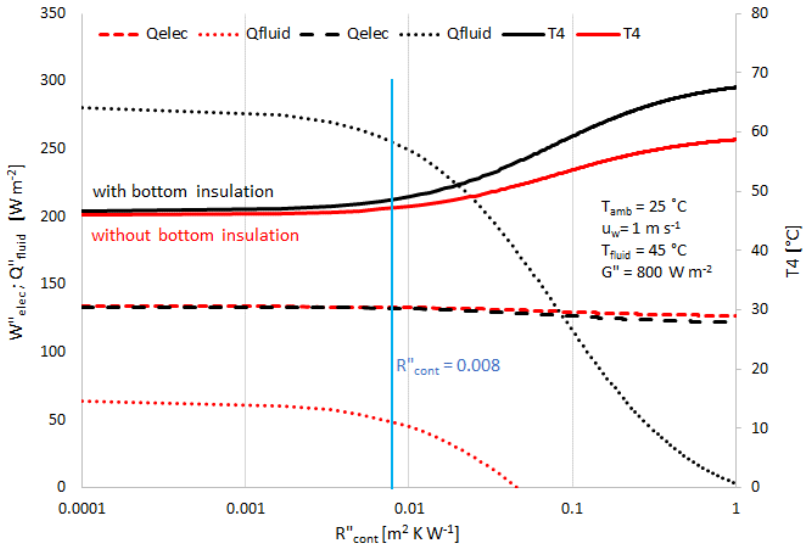

Fig. 13: Contact resistance influence on the electric power generation, thermal energy generation and average solar cells temperature.

4. Conclusions

The present paper showed a new concept of heat exchanger made of corrugated PP to be used in common PV panels, converting them into hybrid solar collectors. This heat exchanger presents simple manufacture and installation as well low final cost. Both in experimental and simulations, water circulates inside multiple channels of the heat exchanger with the main objective to remove heat from the hot surface passing it to the water. The heat removed decreases the PV module operating temperature maintaining it in values closer to water inlet temperature, increasing up to 8% PV efficiency.

The experimental tests were carried out utilizing the indoor PVT heat exchanger test bench. This test bench has components that control water mass flow rate, water inlet temperature and heat flux applied. Nonetheless, just the last two were varied in a specific range to assess the polymeric heat exchanger performance.

After carrying out a combination of experimental tests using different heat fluxes and water inlet temperatures, the thermal contact resistance of 0.008 m^2 K W^{-1} was found out. This result was utilized in simulations encompassing the PVT heat exchanger test bench energy balance. These simulations showed that the thermal resistance circuit can estimate the heat flux absorbed by water circulating inside the PP heat exchanger. The difference between measured and calculated heat fluxes were on average 12% and 8% for experimental configurations without and with bottom thermal insulation, respectively.

With the simulation model validated with the experimental results, a PVT was simulated in a parametric analysis. It was shown that the fluid temperature circulating through the PVT has a major influence on the solar cell temperature. If water is at high inlet temperature about 60 °C, the electricity generation is decreased due to the PV conversion efficiency losses of 7%, on average. However, if water is entering at a lower temperature than that or near the ambient temperature, the electrical efficiency is increased 4%, on average.

The installation of thermal insulation causes a considerable reduction in the amount of heat lost to the environment by convection, then the thermal insulation decreases significantly the influence of wind speed in heat loss and improves the amount of heat absorbed by water. Without bottom thermal insulation, as wind speed increases, the

heat exchanger performance decreases significantly. The use of the bottom thermal insulation is essential for domestic hot water applications, where the temperature difference between the desired water and ambient temperatures are usually above 20 °C. For applications at lower temperatures, like pool heating, the bottom insulation can be dismissed.

The influence on the thermal contact resistance was analyzed and the obtained value of 0.008 m^2 K W^{-1} was considered appropriate for a good thermal and electric generation efficiency.

In future works, the authors will carry out tests using an outdoor PVT test bench, where the PP heat exchanger will be submitted to real weather conditions and its ability to heat water for domestic hot water use and for pool heating will be checked. The heat exchanger performance analysis will be expanded to annual simulations in different regions to assess the economic viability of the proposed heat exchanger.

5. Acknowledgments

This work was developed in R&D Project PD 00403 0049/2020 funded by the Research and Development Program of the National Agency of Electrical Energy (ANEEL) and Engie Brasil Energia S.A. The authors are grateful to the funders ANEEL and Engie and to the LEPTEN laboratory of the Federal University of Santa Catarina (UFSC), the Graduate Program in Mechanical engineering (POSMEC), Advanced Institute of Technology and Innovation (IATI) and Soluz Energia.

6. References

Al-Waeli, A. H. A., Kazem, H. A., Chaichan, M. T., Sopian, K., 2109. Photovoltaic/Thermal (PV/T) Systems: Principles, Design, and Applications, first ed. Springer International Publishing, Switzerland.

Blakesley, J. C., Huld, T., Müllejans, H., Gracia-Amillo, A., Friesen, G., Betts, T. R., Hermann, W., 2020. Accuracy, cost and sensitivity analysis of PV energy rating. Solar Energy, 203, 91–100.

Busson, B. O., Santos, L. O., Carvalho, P. C. M., Carvalho Filho, C. O., 2021. Experimental Assessment and Modeling of a Floating Photovoltaic Module with Heat Bridges. IEEE Latin America Transactions, 19 (12), 2079–2086.

Chow, T. T., 2010. A review on photovoltaic/thermal hybrid solar technology. Applied Energy. 87, n. 2.. 365–379.

Da Rocha, N. M. M., Brighenti, L. L., Passos, J. C., Martins, D. C., 2019. Photovoltaic Cell Cooling as a Facilitator for MPPT. IEEE Latin America Transactions, 17(10), 1569–1577.

Dubey, S., Sarvaiya, J. N., Seshadri, B., 2013. Temperature dependent photovoltaic (PV) efficiency and its effect on PV production in the world - A review. Energy Procedia, 33, 311–321.

Duffie, J. A., Beckman, W. A., 2006. Solar engineering of thermal processes, third ed. John Wiley & Sons, New Jersey.

Enaganti, P. K., Nambi, S., Behera, H. K., Dwivedi, P. K., Kundu, S., Imamuddin, M., Srivastava, A. K., Goel, S., 2020. Performance analysis of submerged polycrystalline photovoltaic cell in varying water conditions. IEEE Journal of Photovoltaics, 10(2), 531–538.

Herrando, M., Ramos, A., Zabalza, I., Markides, C. N., 2019. A comprehensive assessment of alternative absorber-exchanger designs for hybrid PVT-water collectors. Applied Energy, 235, 1583–1602.

Huide, F., Xuxin, Z., Lei, M., Tao, Z., Qixing, W., Hongyuan, S., 2017. A comparative study on three types of solar utilization technologies for buildings: Photovoltaic, solar thermal and hybrid photovoltaic/thermal systems. Energy Conversion and Management, 140, 1–13.

Kaewchoothong, N., Sukato, T., Narato, P., Nuntadusit, C., 2021. Flow and heat transfer characteristics on thermal performance inside the parallel flow channel with alternative ribs based on photovoltaic/thermal (PV/T) system. Applied Thermal Engineering, 185, 1-22.

Kazemian, A., Hosseinzadeh, M., Sardarabadi, M., & Passandideh-Fard, M., 2018. Effect of glass cover and

working fluid on the performance of photovoltaic thermal (PVT) system: An experimental study. Solar Energy, 173, 1002–1010.Kim, J. H., Kim, J. T., 2012. The Experimental Performance of an Unglazed PVT Collector with Two Different Absorber Types. International Journal of Photoenergy, 2012, 1-6.

Kim, J. H., Kim, J. T., 2012. The experimental performance of an unglazed PV-thermal collector with a fully wetted absorber. Energy Procedia, 30, 144–151.

Kumar, P., Singh, A. K., Sudhakar, K., Gupta, V., 2016. Cooling techniques on the flat plate solar photovoltaic-thermal systems: An overview. International Journal of Engineering & Science Research, 6(8), 184-191.

Lamnatou, C., Chemisana, D., 2017. Photovoltaic/thermal (PVT) systems: A review with emphasis on environmental issues. Renewable Energy, 105, 270–287.

Moharram, K. A., Abd-Elhady, M. S., Kandil, H. A., El-Sherif, H., 2013. Enhancing the performance of photovoltaic panels by water cooling. Ain Shams Engineering Journal, 4(4), 869–877.

Ramschak, T., 2020. Existing PVT systems and solutions: IEA SHC Task 60 | PVT systems. Solar heating and cooling programme: Intenational Energy Agency.

Pinho, J. T., Galdino, M. A., 2014. Manual de engenharia para sistemas fotovoltaicos, CEPEL-CRESESB, Rio de Janeiro.

Preet, S., 2018. Water and phase change material based photovoltaic thermal management systems: A review. Renewable and Sustainable Energy Reviews, 82, 791–807.

Shyam, G. N. Tiwari, and I. M. Al-Helal, 2015. Analytical expression of temperature dependent electrical efficiency of N-PVT water collectors connected in series. Solar Energy, 114, 61–76.

Sultan, S. M., Efzan, M. N. E., 2018. Review on recent Photovoltaic/Thermal (PV/T) technology advances and applications. Solar Energy, 173, 939–954.

Suman, S., Khan, M. K., Pathak, M., 2015. Performance enhancement of solar collectors - A review. Renewable and Sustainable Energy Reviews, 49, 192–210.

Zarrella, A., Emmi, G., Vivian, J., Croci, L., & Besagni, G., 2019. The validation of a novel lumped parameter model for photovoltaic thermal hybrid solar collectors: a new TRNSYS type. Energy Conversion and Management, 188, 414–428.